Available online at www.sciencedirect.com
SCIENCE DIRECT®
Polymer Degradation and Stability 84 (2004) 49–60
Polymer Degradation and Stability
www.elsevier.com/locate/polydegstab

Influence of metals on the phenol–formaldehyde resin degradation in friction composites

Monika Křístková[a,*], Peter Filip[b], Zdeněk Weiss[a], Rudolf Peter[c]

[a]*Institute of Materials Chemistry, Technical University Ostrava, Czech Republic*
[b]*Center for Advanced Friction Studies, Southern Illinois University Carbondale, IL, USA*
[c]*Faculty of Nature Science, University of Ostrava, Czech Republic*

Received 2 July 2003; accepted 7 September 2003

Abstract

Degradation process and influence of metal particles (Cu, Fe, CuZn) on the stability of acid catalyzed (novolak) phenolic resin during curing and friction process in friction composites have been studied. Using TGA, FTIR and Py-GC methods, the significant influence of copper and iron chips, in case of high metal concentrations, on degradation process during curing of novolac phenolic resin has been found. The same behavior was confirmed for friction process. It follows that copper and iron can act as catalysts and therefore the model mechanisms for metal catalysis were proposed. The key role in the phenolic resin degradation process belongs to the elimination of formaldehyde, as an important curing agent, caused by metal and metal oxide catalysis. Brass (CuZn) does not influence the stability regardless of concentration but the wear characteristics after friction process of brass containing samples were extremely high if compared to other ones. Brass influence is rather physical as chemical owing to formation of ZnO and consequent degradation of fiber/resin interface. This caused that CuZn particles were released from the matrix and a high porosity on the friction surface was observed.

Keywords: Phenol-formaldehyde resin; Friction composite; Thermal degradation

1. Introduction

In the production of composites, both acid (novolak) and base (resole) catalyzed phenolic materials are used. In this application, phenolic resin is used as matrices to protect and reinforce the fibers contained within the composite structure.

The large numbers of studies have been carried about degradation studies of phenol formaldehyde resin [1–13].

1.1. Inert atmosphere

The three stages of gas production and the structural change of the residual carbonaceous material of phenol-formaldehyde resin is considered to be as follows:

In the first step (<450 °C), the carbonaceous material of the phenolformaldehyde resin contains structures such as diphenylether, benzene nuclei bonding with methylene bridges [3,8]. In this stage mainly H_2O evolves, arising from condensation reaction between phenolic groups.

In the second step (450–700 °C), the benzene nuclei combine directly with one another as biphenyl, by the breaking of $–CH_2-$ bridges and –O- bridges. Mainly in the 500–560 °C range, the drastic changes occur in that the network collapses [11]. In this step, the decomposition of bridges producing some unpaired electrons and the direct bonding of benzene nuclei take place simultaneously. The larger gas evolution and the greatest loss of weight occur. The reactions occurring in this stage are: cracking, dehydration, dehydrogenation [7]. At 500 °C, carbonyl groups have been detected during resin degradation process, although degradation was taking place in an inert atmosphere, thus leading to the conclusion that an auto-oxidation process of the methylene bridges occured. Water and $^{\bullet}OH$ radicals may also act as a source of oxygen [3].

In the third step (700–1000 °C), the remaining hydrogen atoms are removed as H_2 as a dominant product and

* Corresponding author. Tel.: +42-59-699-1640.
E-mail address: monika.kristhova@email.cz (M. Křístková).

0141-3910/$ - see front matter © 2004 Elsevier Ltd. All rights reserved.
doi:10.1016/j.polymdegradstab.2003.09.012

results from the splitting of hydrogen atoms directly bonded to benzene nuclei. At the same time, the size of aromatic nuclei increases suddenly by the partial rearrangement accompanying the strong three-dimensional bonding among them [8]. The loss of weight is very slow. Furthermore, condensation reactions of the aromatic rings happen to form polycyclic aromatic system [2].

The process of carbonization is completed at 900 °C. Between 500 and 800 °C the destruction of crosslinks leads to the formation of clusters of the aromatic units [7].

1.2. Air

Oxidation is caused by oxygen from the atmosphere and it usually starts at lower temperature (300 °C) than when the resin was heated in an inert atmosphere [3]. Carbonyl groups were detected and it led to the deduction that methylene bridges are the first to be oxidised as the most vulnerable sites, giving a hydroperoxide precursor and benzophenone linkages are formed as can be easily seen in Fig. 1. Upon further heating in air quinones and carboxylic acids are formed (Fig. 2).

The main degradation route of phenol-formaldehyde resins exposed to elevated temperature involves oxidation, regardless of surrounding environment—air, nitrogen or vacuum [3].

Phenol–formaldehyde resin is one of an important component of friction composites used as bonding agent. Although the real friction composites content at least 20 components and interaction between phenolic resin and other parts of composite system can be expected, in this paper the model systems of novolac-type phenolic resin with metal particles (Cu, Fe and CuZn), for simplification, were chosen and mutual interactions between individual metals and phenolic resin during curing and friction processes will be study and discussed.

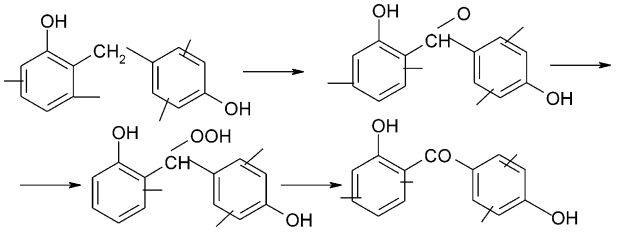

Fig. 1. The formation of carbonyl group (benzophenone structure).

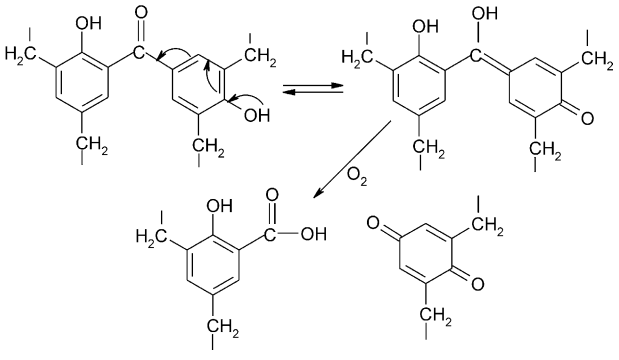

Fig. 2. The formation of quinoid structure and carboxylic group.

2. Experimental

2.1. Materials and sample preparation

Two step phenolic resin HRJ-652 (Schenectady International) with 7–9 wt.% of hexamethylenetetramine and metal chips of Cu, Fe and CuZn (Global Material Technologies) were used for samples preparation. The contents of metal particles were chosen according to appearance in the real composites for friction application. The formulation of investigated samples is given in Table 1.

Samples were prepared in form of pellets with dimensions 57.15 × 10 mm. Following procedures were applied: (1) mixing for 15 min, (2) hot pressing at 170 °C for 30 min, (3) curing in furnace at 170 °C for 5 h in air atmosphere in accordance with supplier.

Samples for TGA, GC-pyrolysis and FTIR were cut by diamond saw (Isomet plus, Buehler) from the cured pellets and ground in the ball mill Fritsch for 10 min. The 10 μm thick surface layers of the samples subjected to friction test were cut by micro knife and used for FTIR analysis.

Table 1
The compositions of investigated resin and resin (PF)/metal samples

Sample notation		Metal content		Notes
		vol%	wt.%	
A	PF	–	–	Noncured
B	PF	–	–	Cured
C	PF + Cu	5	25	Cured
D	PF + Cu	25	68	Cured
E	PF + CuZn	5	24	Cured
F	PF + CuZn	25	67	Cured
G	PF + Fe	20	58	Cured
H	PF-cured	–	–	For friction test
I	PF + Cu-cured	5	25	For friction test
J	PF + Cu-cured	25	68	For friction test
K	PF + CuZn-cured	5	24	For friction test
L	PF + CuZn-cured	25	67	For friction test
M	PF + Fe-cured	20	58	For friction test
N	PF-noncured	–	–	For TGA
O	PF-cured	–	–	For TGA
P	PF + Cu-cured	5	25	For TGA
Q	PF + Cu-cured	25	68	For TGA
R	PF + Fe-cured	20	58	For TGA

2.2. Methods

2.2.1. Friction assessment and screening test (FAST)

Samples H, I, J, K, L, M (Table 1) were subjected to the friction assessment and screening test (Link Engineering, Detroit, MI). In this test, a sample of composite material with dimensions 12.7 × 12.7 × 5 mm is rubbed against the cast iron disc. Constant friction force 77.4 N and constant sliding speed 25 km/h were applied. The friction coefficient was recorded every 5 seconds. Durations of friction tests were 90 min. Light microscopy (LM) observations of friction surafaces were performed using Nikon FX35 microscope (polarized light, analyzer in, retarder plate out). Images from the light microscopy observations were recorded using CCD camera Sony DXC-151A attached to the microscope and Optimas©6.1 image analysis software.

2.2.2. Thermogravimetric analysis (TGA)

The experiments were carried out with samples N, O, P, Q, R (Table 1) on a CAHN TG-171 analyzer with flow control MKS type 247 Device. Different atmospheres were used: 1) purge gas (in weight system)—Argon with flow 100 cm^3/min, 2) working gas—Air with flow 90 cm^3/min. Mass of the analyzed samples were 200–390 mg. Following temperature program was applied: (1) isothermic process at 25 °C, process last 60 s, (2) dynamic heating from 25 to 500 °C, with heating rate 5 °C/min, (3) dynamic cooling from 500 to 25 °C, with cooling rate 20 °C/min.

Brass containing samples E and F were not analyzed in TGA. Sublimation of ZnO during the temperature process and subsequent condensation on the part of weight and furnace system made measurement and calculation of sample loss complicated. It is necessary to note that also in samples P, Q and R, the presence of metals made calculation of weight loss during TGA in air a complex task since oxide formation accompanied the resin degradation. The contents of metal oxides in metal chips of sample P and Q were analyzed by INEL CPS 120 with position sensitive detector PSD 120. CuK_α radiation (λ = 1.54056 Å), Ge monochromator, Si standard for calibration of detector were used. The samples were analyzed by glass capillary tube method. The duration of analysis was 2000 seconds at applied current 15 mA and voltage 25 kV. For analysis of Fe containing sample (R) MoK_α radiation (λ = 0.79495 Å) was used. Using the crystallographic data for Cu, Fe and their oxides, the diffraction patterns for mixtures of metals and oxides in different concentrations were calculated [14]. Calculated and observed XRD patterns were compared by X-ray quantitative phase analysis (XQPA) program [15] and vol.% of oxides were determined.

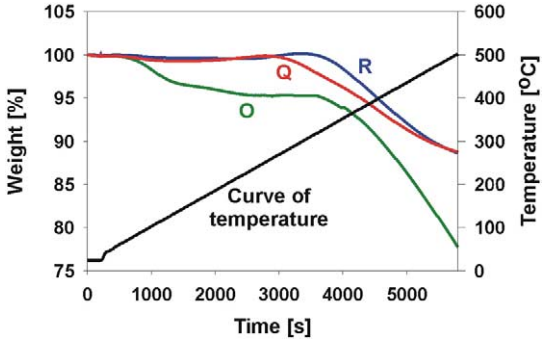

Fig. 3. TG measurement of samples O (PF-cured), Q (PF + 25 vol.% Cu) and R (PF + 20 vol.% Fe).

2.2.3. Gas chomatography–pyrolysis analysis (Py-GC–MS)

In this present work the, Py-GC–MS method for pyrolysis products of samples A, B, C, D, E, F, G was used. Several 0.1 – 0.4 milligrams of samples were pyrolyzed in furnace coupled to Hewlet Packard 5890 chromatograph. The two pyrolysis temperatures 400 and 800 °C were used, and the duration of pyrolysis was 20 seconds. The compounds were separated in 50 m capillary column with 0.2 mm diameter. The stationary phase was DB-5MS (layer 0.33 μm). The column temperature was programmed at a rate of 5 °C/min and varied from 40 to 300 °C. The mass spectrometry detector with quadruple analyzer was used. The carrier gas was He. Differences in evolving of compounds from samples A–G were evaluated by analysis of principal components. The principals of this method are described in [16].

2.2.4. Infrared analysis (FTIR)

Samples A to R (Table 1) were analyzed by FTIR spectrometer Avatar 320 NICOLET with KBr pellet method. The amounts of samples were approximately 0.001 g and the rest to 0.2 g was KBr. A sample homogenization process was performed in a mortar. The moisture water was removed using an attached vacuum pump. The samples were pressed to the pellet form by press NICOLET. The pressure was 527 MPa. The diameter of pellet was 13 mm.

3. Results and discussion

3.1. Thermogravimetry

The thermograms of the novolacs sample O, Q, R under air flow are given in Fig. 3. Weight loss at the sample O appears in two steps. The first step occurs at 170 °C and corresponds to the polycondensation reaction. After this initial weight loss of about 5%, the sample does not lose weight till 340 °C. This stabilization can be explained by the fact that, new structures can be formed during oxidation. These structures are stable until the temperature is high enough and the whole polymer structure collapses [3]. The second

Table 2
The sumary results of oxides (vol.%) and weight loss of resin after TGA

Sample	N	O	P	Q		R
Oxides	–	–	Cu_2O	Cu_2O	CuO	Fe_2O_3
Volume percentage [%]	–	–	6.5	23.0	2.0	45.0
weight loss of resin determined by TGA [%]	18.36	21.88	20.97	11.05		11.33
weight loss of resin calculated [%]	–	–	28.09	40.25		39.17

weight loss at 340 °C is caused by oxidative resin degradation. The corresponding weight loss until 500 °C is 22%. The thermal behavior of samples Q and R is similar, however differs from the sample O. The first weight loss owing to oxidic layers formation is not evident. The final weight loss occurs at lower temperatures (270 °C for sample Q and 300 °C for sample R) when compared to sample O.

Hematite Fe_2O_3 was determined in the sample R (Table 2). In the sample P, the cuprite Cu_2O (Table 2) was identified, while in the sample Q the cuprite and tenorite CuO were identified (Table 2).

Comparison of the mass loss of resin calculated and determined by TGA is given in Table 2. According to Table 2, the greatest mass loss (40.25%) was calculated for the sample Q (PF + 25 vol.% Cu). Sample R (PF + 20 vol.% Fe) behaves in a similar fashion with weight loss slightly lower (39.17%). The weight loss for pure cured resin sample (O) until 500 °C was 22%, as it follows from Fig. 3. It follows that copper and iron significantly influence the mass loss of phenol–formaldehyde resin. Brass containing samples were not analyzed in TGA owing to ZnO sublimation during the temperature process and subsequent condensation on the part of weight and furnace system, which made measurement and calculation of sample loss complicated. Owing to this fact, the mass losses of brass containing samples are not known and it is impossible to compare these with copper and iron containing samples. Percentages of mass loss represented a degradable part of resin exposed to 500 °C. In real friction composite samples a degradable part of resin corresponds to friction layer. As it is easily seen from Table 2, the values of resin weight loss determined by TGA compared to calculated ones can differ by 30%.

3.2. Gas chromatography – pyrolysis

Among the pyrolysis products up to 400 °C of novolac resin 10 volatile compounds (phenol, *o,p*-cresol, benzodioxan, 2,2′ a 4,4′-metylenbisphenol), were detected and three of those were not identified. Two phenols with two retention times were found. The first belongs to the free phenol entrapped in cured resin system, while the second one is evolved with elevated temperature.

After the pyrolysis up to 800 °C the 70 identified compounds and seven were not identified. New compounds as benzene, toluene, *o,m,p*-xylenes, benzofurane, di and tri-methylphenols, biphenyl and polyaromatic compounds like naphtalene, anthracene, fenanthrene, fluorene, xanthene, pyrene or fluoranthene and their derivatives appeared. Temperature higher than 400 °C makes possible the formation of the aromatic compounds such benzene, toluene and xylenes. Samples D (PF + 25 vol.% Cu) and G (PF + 20 vol.% Fe) demonstrate the highest percentage concerning the release of compounds without the hydroxyl attached to the aromatic ring such as benzene, toluene, *o,m,p*-xylens and 1,1′-methylenebisbenzene. The loss of hydroxyl from aromatic ring is necessary requirement for the formation of these compounds [2]. Owing to this fact that from samples D and G these compounds are evolved in the highest amounts, it can be attributed to the influence of copper and iron on this part of resin degradation process.

Characteristic products with condensed rings are fluorene, dibenzofurane, 9H-xanthene, benzonaphtofurane, anthracene, phenanthrene and can be created in a cyclization reaction with the participation of hydroxyl [6] or methyl [8] groups in an ortho position to methylene bridges.

The 54 (compounds with retention time $\geqslant$29 min) of 77 released compounds were used for principal components analysis. Components are new hypothetic variables explain system variability. The covariance matrix, its eigen values and corresponding eigenvectors (coefficients of principal components) were calculated. Percentage of variability for each principal component was determined. As can be seen from Table 3, the three components due to three highest eigen values were chosen. The sum of variability of three principal components is 95.65%. The values of three principal components for samples A–G are given in Table 4. The value for each principal component was calculated as sum of linear combinations of experimentally determined value and eigenvector value. The graphs of principal components dependences were created and are shown in Figs. 4 and 5.

Table 3
The percent of variability for three principal components

Components	1	2	3	Σ
Percent of variability [%]	68.14	19.61	7.90	95.65

The axes of coordinate system cross in the directions of maximal points group. The compounds showing the strongest influence on the first three principal components according to values of eigenvectors of variables at three principal components [3D distance from (000)], were determined:

1. 2,2′-methylenebisphenol
2. 4-phenylethenylphenol
3. 2,3-dihydro-2-methylbenzofuran
4. 9H xanthene-9-on.

The first principal component can be interpreted as a factor of 2,2′-methylenebisphenol. This compound proves the strongest influence on system variability. Sample A (PF-noncured) has the highest value of the first principal component. This compound (oligomer) [17] is present in novolac before curing process and with increasing temperature is further evolved [2]. Curing process in sample A occurred during pyrolysis and compound 1 is evolved. Compound **4**—phenylethenylphenol has the strongest influence on the second component. The highest value of this component exhibited sample D (PF + 25 vol.% Cu). Compounds **3** and **4** have the same influence on the third component. This component is important to distinguish sample G (PF + 20 vol.% Fe). Points A, D (Figs. 4 and 5) and G (Fig. 5) are apparently separated from the group of other points. This fact demonstrates the different behavior concerning of compounds evolving.

Table 4
The values of three principal components for samples A–G [A (PF-noncured), B (PF-cured), C (PF + 5 vol.% Cu), D (PF + 25 vol.% Cu), E (5 vol.% CuZn), F (25 vol.% CuZn), G (PF + 20 vol.% Fe)]

Sample	A	B	C	D	E	F	G
Component							
1	4.59	−0.22	−0.41	−4.22	0.47	−1.02	1.51
2	0.82	−0.64	−1.27	1.68	−1.51	0.49	−0.84
3	0.25	0.30	1.01	−0.31	0.19	0.35	−1.83

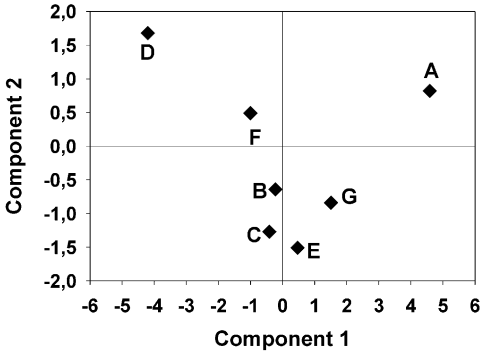

Fig. 4. Dependence of component #2 on component #1.

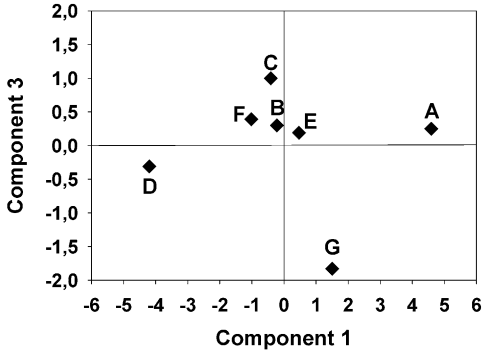

Fig. 5. Dependence of component #3 on component #1.

Samples D (PF + 25 vol.% Cu) and G (PF + 20 vol.% Fe) demonstrated the highest percentage (compared to other samples) concerning the release of compounds without the hydroxyl attached to the aromatic ring such as benzene, toluene, *o,m,p*-xylens and 1,1′-methylenebisbenzene. Owing to fact that loss of hydroxyl group from aromatic ring is necessary requirement for the formation of these compounds, it can be connected with the influence of copper and iron on this part of degradation process of resin. The hydroxyl radical, in turn, would represent a source of oxygen for further oxidation reactions.

3.3. Infrared analysis

IR dependencies as detected for samples A (PF-noncured) and B (PF-cured) are shown in Fig. 6.

The interpretation of identified bands of infrared spectra is summarized in Table 5.

The bands of spectrum B- PF-cured (Figs. 6 and 7) decrease due to condensation. In these spectra the two new absorptions increase. 1650 cm^{-1} (Fig. 7) as a weak shoulder on the 1600 cm^{-1} doublet and can be ascribed to carbonyl groups (benzophenones) produced trough oxidation reaction. As a consequence of condensation reaction, ethers are formed and evidence of this is found in the growing band at 1252 cm^{-1} (Figs. 6 and 7) that was absent in spectrum A.

In cured samples (B, C, E) the OH stretching band at 1237 cm^{-1} shifts towards higher wave numbers (Fig. 6) because changes take place in the H bonding and the number of OH groups decreases. This is probably due to condensation processes and crosslinking [3]. Also, the 1372 cm^{-1} OH band decreases in intensity (Fig. 6) for the same reasons. The absorption at 1237 cm^{-1} is due to phenolic OH and CO stretching respectively. The relative intensities of two peaks 1610 and 1595 cm^{-1} (doublet aromatic ring stretching) at A (1595 > 1610 cm^{-1}) and at B (1595 < 1610 cm^{-1})—see Fig. 6, are reversed due to changes in the ring substitution, probably because of crosslinking [3]. Indications of these changes can also be found in the growing band at 885 cm^{-1} (Fig. 7) belonged to tetra and other higher

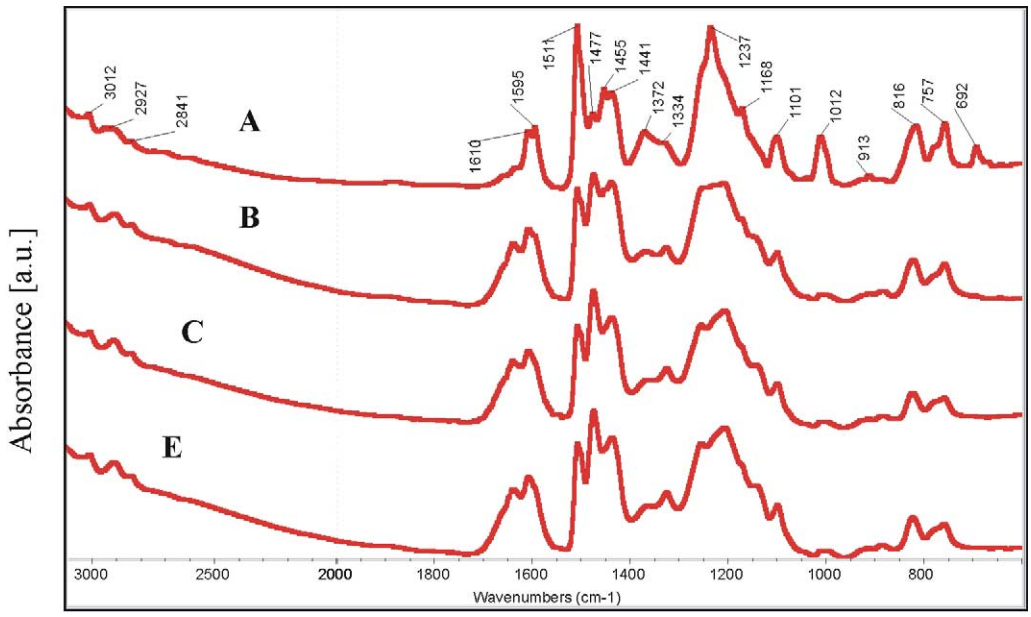

Fig. 6. FTIR spectra of samples A (PF-noncured), B (PF-cured), C (PF + 5 vol.% Cu) and E (PF + 5 vol.% CuZn) after curing process.

Table 5
Infrared bands and assignments for the HRJ-652 resin (br. = broad; w. = weak; m. = medium; s. = strong)

Band position [cm^{-1}]	Charact.	Assignment	References
3016	w.	aromatic CH stretching	[3]
2927	w.	aliphatic CH_2 asymetric stretching, CH_3	[3]
2837	w.	aliphatic CH_2 symetric streching	[3]
1720 – 1740	w.	carboxylic group	[2]
1650	m.	benzophenone	[3]
1610	s.	ring stretching (1,2,4)	[3]
1595	s.	ring stretching	[3]
1510	s.	semicircle ring stretching (1,2,4)	[3]
1476	m.	tetra substituted ring	[3,5]
1455	m.	semicircle ring stretching (1,2,4)	[3]
1440	m.	aliphatic CH_2 scissor bending	[3]
1371	w.	OH, stretching CH_3	[3]
1334	w.	CH_3 attached to the aromatic ring	[3]
1250	s.	ether	[3]
1236	s.	OH, CO stretching	[3]
1171	m.	2-and/or 4-substituted ring	[3]
1101	m.	in plane ring deformation (1,2,4)	[3]
1012	m.	CH_3 attached to the aromatic ring	[3,18]
912	w.	aliphatic CH_2 wagging	[3]
881	w.	tetra substituted (1,2,4,6) ring	[3,10]
816	m.	out of plane ring deformation (1,2,4)	[3]
756	m.	out of plane ring deformation (1,2,6)	[3]
691	m.	mono substituted benzene ring	[3]

substitutions. Peak of 1510 cm^{-1} (1,2,4-tri substituted ring) decrease (Figs. 6 and 7), while 1476 cm^{-1} indicating tetra-substituted ring increase (Fig. 7). Tri-substituted ring is changed to tetra-substituted ring during curing process.

Absorbance of peaks at 1101 and 816 cm^{-1} belongs to the 1,2,4-trisubstituted ring. The peak at 1168 cm^{-1} corresponds to the 2 and/or 4-substituted ring. This absorption decreases too (Fig. 6). Peaks 1012, 2927 a 1334 cm^{-1} (Fig. 6) are the bands of CH_3 group attached to the aromatic ring. Absorption of 1012 cm^{-1} decreases due to curing process and fragmentation reaction. Band 1334 cm^{-1} is decreasing too (Fig. 6), but after curing process this band remains as 1327 cm^{-1} (Fig. 7), that is still significant on account of decreasing of neighbouring band 1371 cm^{-1} belonged to OH group [3]. Methyl deformation bands usually appear at about 1460 cm^{-1}, but in this case are hidden by the 1455 cm^{-1} aromatic ring stretching [3]. The bands of methylene group are at 913, 1440, 2927, 2840 cm^{-1} but especially band 1440 cm^{-1} is significant (Fig. 7) because of methylene links formation during curing process. Peak 692 cm^{-1} (Fig. 6) belonged to monosubstituted ring disappears, because of higher substituted ring formation in curing process.

IR spectra of samples C, E and F are similar to spectrum of sample B (Figs. 6 and 7), only bands 1475 cm^{-1} (tetrasubstituted ring) and 1250 cm^{-1} (ether) are more significant (Figs. 6, 7). The spectrum of sample D—PF + 25 vol.% Cu (Fig. 7) is different. Absorption of all bands are lower than at sample B, some bands 3013, 2913, 2827 cm^{-1} which belonged to the C–H bond, disappeared. Peak 1632 cm^{-1} (Fig. 7) is residue of peaks

1650 cm^{-1} (benzophenon) and 1610, 1595 cm^{-1} (doublet arom. ring). The residues of peaks belonged to the trisubstituted and tetrasubstituted benzene ring are represented by band 1474 cm^{-1}. The last visible band in Fig. 7, 1213 cm^{-1} incorporates the residues of bands corresponding to ether and trisubstituted benzene ring. In this spectrum the characteristic absorptions belong to the aromatic system remained only. Spectrum of the sample G—PF + 20 vol.% Fe (Fig. 7) has the same bands as sample D, but the absorptions of all bands are slightly stronger compared to spectrum of sample D.

Spectra I (PF + 5 vol.% Cu) and K (PF + 5 vol.% CuZn) have similar character as spectrum of sample H (PF-cured)—see Fig. 8. The 1510–1400 cm^{-1} and 1255 – 1100 cm^{-1} regions grow in complexity as can be seen at spectra of samples M (PF + 20 vol.% Fe), J (PF + 25 vol.% Cu) in Fig. 9 or at O (PF-cured), P (PF + 5 vol.% Cu) in Fig. 10. The OH bands at 1370 cm^{-1} decrease further while all the bands become more complex, showing that main structure of the polymer is still there but changing towards a polyaromatic structure. This can be seen by observing the 1600 cm^{-1} band that was originally a sharp doublet but becomes a broad band covering a range of ca 100 cm^{-1}, typical for poly-aromatic system [3]. However, a new absorption appears in this case as a shoulder at 1683 cm^{-1} (Figs.

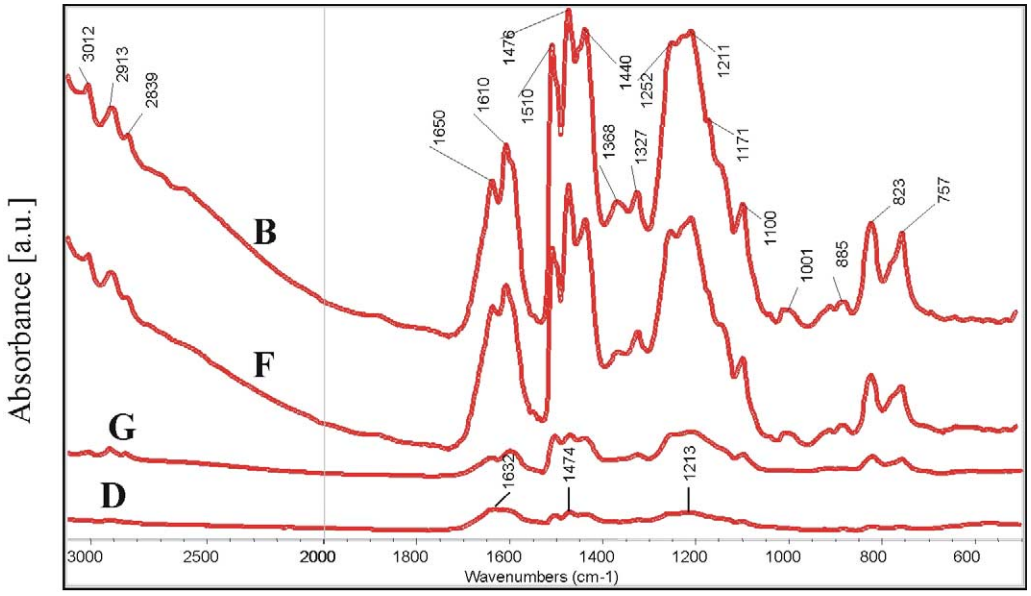

Fig. 7. FTIR spectra of samples B (PF-cured), D (PF + 25 vol.% Cu), F (PF + 25 vol.% CuZn) and G (PF + 20 vol.% Fe) after curing process.

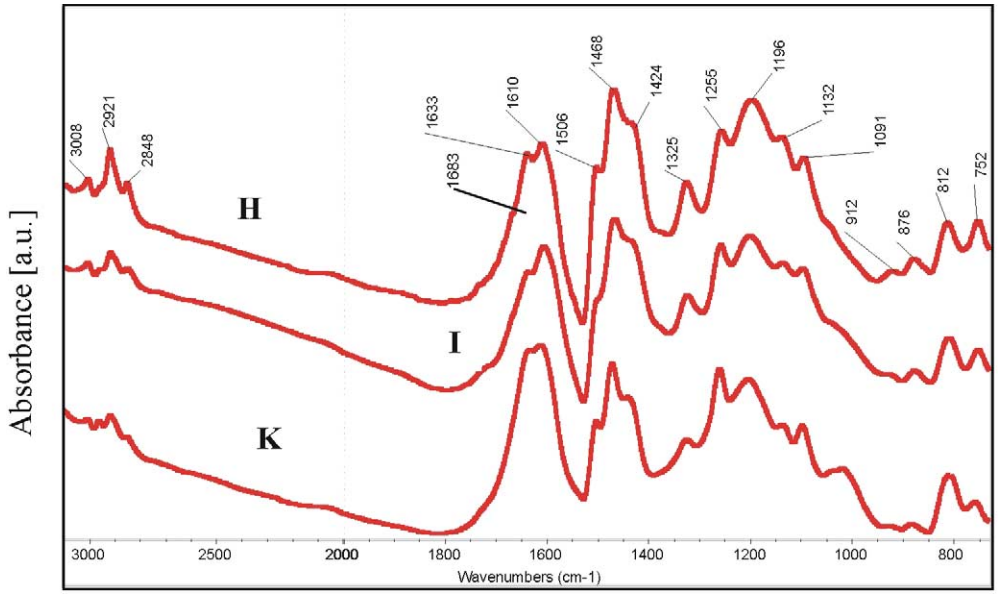

Fig. 8. FTIR spectra of samples H (PF-cured), I (PF + 5 vol.% Cu) and K (PF + 5 vol.% CuZn) after friction test.

8–10) due to quinoid structure formed after the oxidation of the methylene bridges. The 1650 cm^{-1} absorption of the carbonyl group is present but difficult to detect because it is hidden by the quinoid band and the 1600 cm^{-1} doublet [3]. Also the band at 1255 cm^{-1} ether band due to oxidation, becomes more intense. Evidence of oxidation is also given by the new weak absorption growing at 1710–1740 cm^{-1} due to carboxylic acid as can be seen in spectra of samples M, J (Fig. 9) and O, P, R (Fig. 10).

Spectra interpretation of metal containing samples (I, J, K, L, M—after friction process) can be complicated by the fact that part of resin char can be removed as wear during friction process. Than the friction process is performed predominantly on the metal particles without resin participation. The sample surface temperatures owing to sample morphology can vary in the range 300 – 900 °C and therefore degree of degradation can be different in every part of the friction surface. This effect can be caused by sample preparation too. The thickness of the friction layer can vary and the bulk resin with a lower degree of degradation can be removed into sample for FTIR analysis. Therefore, during friction process the resin degradation seems not to be as extensive when

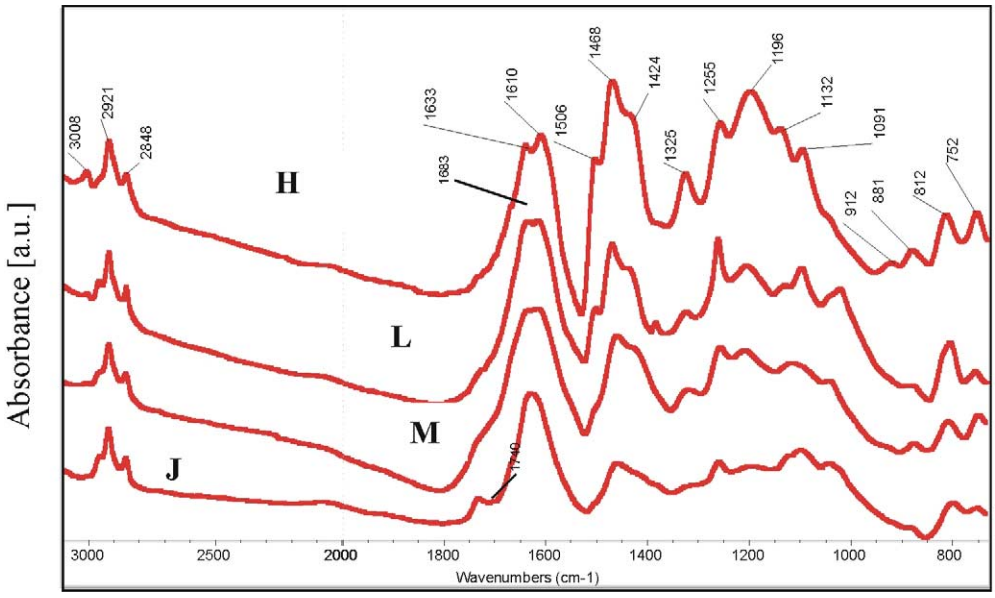

Fig. 9. FTIR spectra of samples H (PF-cured), J (PF + 25 vol.% Cu), L (PF + 25 vol.% CuZn) and M (PF + 20 vol.% Fe) after friction test.

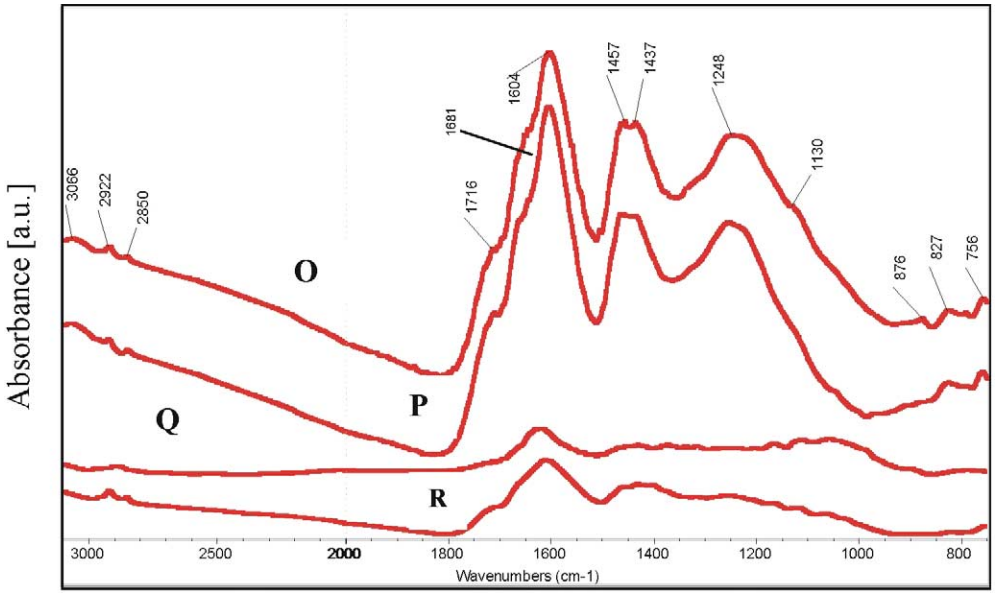

Fig. 10. FTIR spectra of samples O (PF-cured), P (PF + 5 vol.% Cu), Q (PF + 25 vol.% Cu) and R (PF + 20 vol.% Fe) after TGA analysis.

compared to TGA in spite of higher temperature on the friction surface.

The most significant changes in spectra of samples D (PF + 25 vol.% Cu), G (PF + 20 vol.% Fe)—after curing process, J (PF + 25 vol.% Cu), M (PF + 20 vol.% Fe)—after friction process, Q (PF + 25 vol.% Cu) and R (PF + 20 vol.% Fe)—after TGA appeared, as it is evident from Figs. 7, 9 and 10. These changes are the most significant after curing process at spectra of samples D (PF + 25 vol.% Cu), G (PF + 20 vol.% Fe) and after TGA at spectra of samples Q (PF + 25 vol.% Cu), R (PF + 20 vol.% Fe). These results can be connected with influence of copper and iron on degradation process of phenol–formaldehyde resin. Although samples during the curing process were exposed to 170 °C, the resin (samples D and G) seemed to be exposed to a higher temperature than 170 °C. Brass (CuZn) did not influence the degradation regardless of concentration. Spectra interpretation of metal containing samples (I, J, K, L, M—after friction process) were complicated by the fact that part of resin char was removed as wear during friction process. Than the friction process was performed predominantly on the metal particles without resin participation.

3.4. Model mechanisms for metal and metal oxides catalysis

Using TGA, FTIR and Py-GC methods, the significant influence of copper and iron chips, in case of high metal concentrations (25 vol.%), on degradation process during curing of novolac phenolic resin was found. The same behavior was confirmed for friction process, too. It follows that copper and iron can act as a catalysts. Brass did not have the impact on the phenolic resin degradation during curing regardless of concentration, as is evident from Sections 3.1.–3.3.

3.4.1. Metal catalysis

Formaldehyde can be oxidized in presence of metals or their ions. In such heterogenous system as the phenol – formaldehyde resin with metal particles is, formaldehyde represents a mobile phase, it can move to the metal/phenolic resin interface where the catalytic processes take place.

Formaldehyde can be generated if two methylol groups react under acidic conditions with one another to form an ether linkage. Dibenzyl ethers are not so stable and at temperature above 150 °C they undergo a

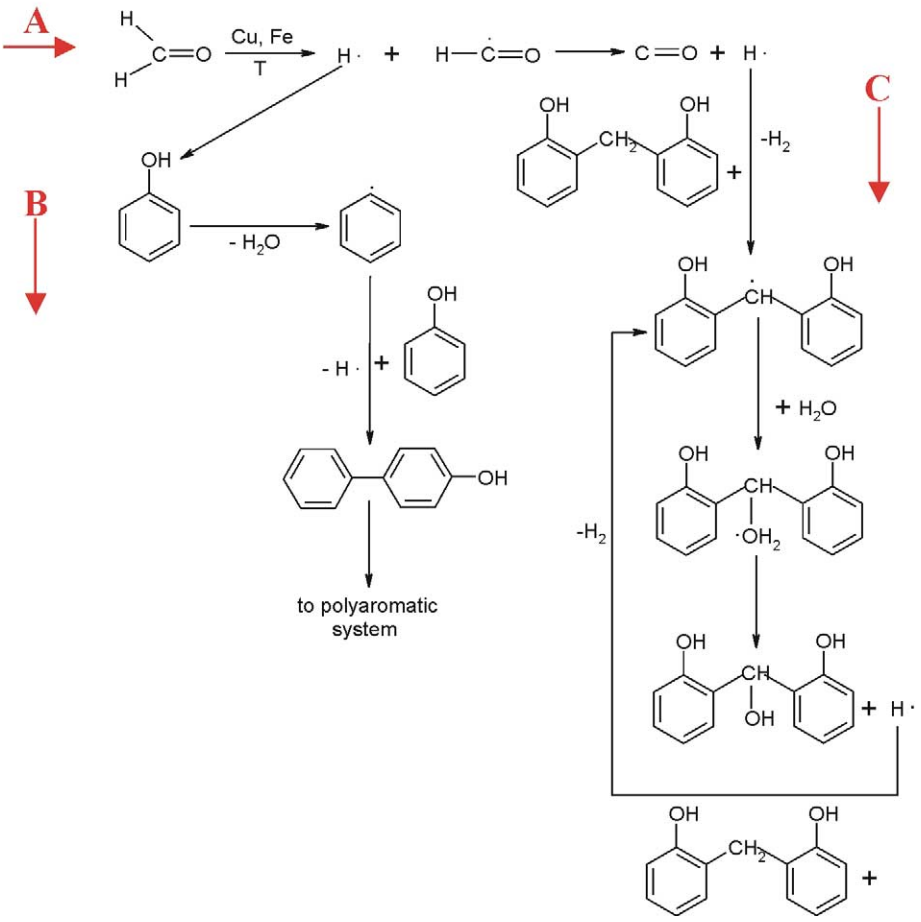

Fig. 11. Proposed degradation reaction of phenol-formaldehyde resin with using copper and iron as catalysts.

breakdown of ether links to give methylene links with loss of formaldehyde [1]. Another reaction for formaldehyde releasing is its evolving by HEXA decomposition during crosslinking process.

The possible degradation process of phenol-formaldehyde resin using copper and iron as catalysts is proposed in Fig. 11.

Oxidation of formaldehyde in presence of copper or iron, results in formation of carbon oxide (CO) and liberation of hydrogen radicals [19]. Free hydrogen radicals may participate in several other reactions as indicated in **route A** in Fig. 11.

Releasing hydrogen radical can support the cleavage of hydroxyl from phenol and form phenyl radical with evolution of water. Phenyl radical can undergo a reaction with another aromatic compound and produce a biphenyl type stucture, which can serve as preproduct for polyaromatic system formation. This process is illustrated as **route B** in Fig. 11.

Another possible is reaction between a hydrogen radical and methylene group accompanied by molecular hydrogen release and it is shown as **route C** in Fig. 11. Methylene linkage in phenol–formaldehyde resin presents site with a high reactivity to radicals owing to the high electron density caused by conjugation with two aromatic nuclei. Consequent reaction of 2,2′-methylenebisphenol radical with water leads to the formation of hydroxyl on the methylene bridge. The newly formed hydrogen radical can react with another methylene group which is accompanied by additional evolution of molecular hydrogen and 2,2′-methylenebisphenol radical formation.

3.4.2. Metal oxide catalysis

Catalytic activity of copper and iron can be also attributed to the presence of Cu^{2+} and Fe^{3+} ions in the surface layers. During the curing process these ions are present on the metal surfaces in form of very thin and probably random oxidic layers. They can serve as catalyticaly active centres.

During a oxidic catalysis, the interaction between O ions and neighboring metal ion is expected. The first step is the dissociative adsorption of alcohol and formation of surface alcoxid [20,21]. Oxidation of methylol group as a part of phenol-formaldehyde molecule can be suggested according to Fig. 12.

The O–M bond present in the surface layer of metal oxide causes weakness of C–H bond belonging to the carbon bearing original hydroxyl group, which simultaneously leads to C=O bond formation. As a result, molecular hydrogen is released and aldehyde is formed.

Another possibility is oxidation of formaldehyde using the oxide surface. Oxidation proceeds in two steps. In the first one, the formaldehyde is oxidized to formic acid. During the second step, the carbon dioxide and water are formed. An example of formaldehyde oxidation on the tenorite (CuO) surface is given in Fig. 13. An analogous formaldehyde oxidation can progress using hematite (Fe_2O_3) as a catalyst.

The catalytic inactivity of brass can be attributed to the presence of zinc in copper lattice. With addition of zinc to copper lattice, the concentration of electrons in primary alloy increases [22]. Consequently, the copper ions Cu^{2+} in surface layers are reduced to catalytically inactive copper form Cu^0 and Cu^+.

However the wear rates of brass containing samples were extremely high if compared to copper and iron containing samples. It can be considered that brass influence is rather physical owing to formation of ZnO and consequent weakening of fiber/resin interface. Owing to this fact, the CuZn fibers were released from the matrix and a high porosity was observed by light microscopy on the friction surfaces, as can be easily seen in Fig. 14.

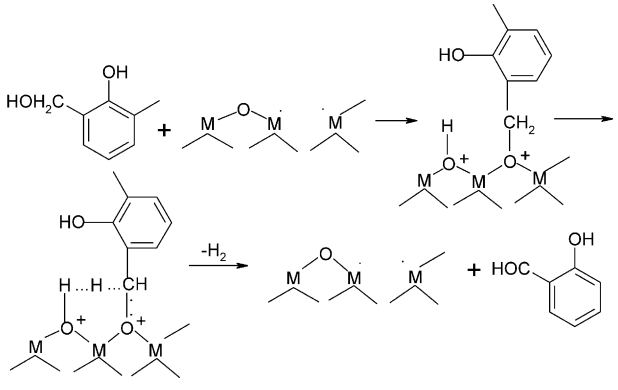

Fig. 12. Oxidation of methylol group using metal (M) oxide as a catalyst.

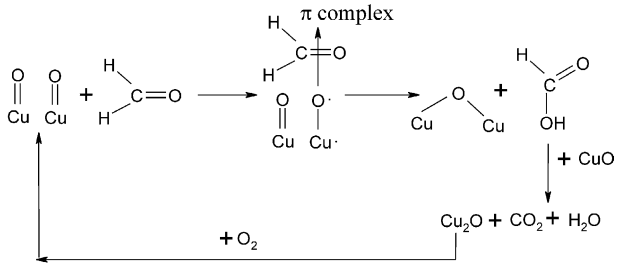

Fig. 13. Oxidation of formaldehyde using tenorite (CuO) as a catalyst.

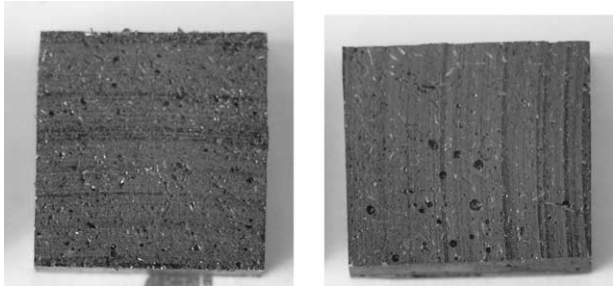

Fig. 14. The friction surface of brass containing samples after friction test observed by light microscopy (LM).

4. Conclusions

Metals (Cu and Fe), in case of high metal concentrations, significantly support degradation process of phenol–formaldehyde novolac resin at curing and friction processes. Their influence can be considered as chemical and they may act as catalysts. Degradation is not evident in the sample with 5 vol.% Cu, it can be connected with quantity of Cu.

Metals and their oxides can catalyze the degradation process of phenol–formaldehyde novolac resin in several ways, as it was proposed in model mechanisms:

- Formaldehyde as important curing agent is oxidized with using of metal or metal oxide as catalysts. Consequently, novolac has a less degree of crosslinking, than the oxygen can better penetrate into the polymer and support the formation of oxidic structures and resin is prone to furthure degradation. Oxidation of formaldehyde in presence of metals, results to the formation of hydrogen radicals, whose may participate in several other reactions.
- Releasing hydrogen radical can support the cleavage of hydroxyl from phenol and form phenyl radical with evolution of water. Phenyl radical can undergo a reaction with another aromatic compound and produces a biphenyl type stucture, which can serve as preproduct for polyaromatic system formation.
- Reaction between hydrogen radical and methylene group of 2,2′-methylenebisphenol. Methylene linkage presents the most vulnarable site with a high reactivity to radicals owing to high electron density caused by conjugation with two aromatic nuclei. Consequent reaction between the 2,2′-methylenebisphenol radical and water leads to the formation of hydroxyl on the methylene bridge as an important step in degradation process of phenol – formaldehyde resin. Hydrogen radical produced as side product of this reaction can react with another methylene group accompanied by evolution of molecular hydrogen together with 2,2′-methylenebisphenol radical formation. Hydroxyl on methylene bridge than can undergo to another oxidation and benzophenone type structure can be formed. Sequence of reactions between the 2,2′-methylenebisphenol radical and water leads to the formation of hydroxyl on the methylene linkage accompanied by releasing of molecular hydrogen.
- Metal oxides catalyze the oxidation of functional groups such as alcoholic or aldehydic groups. As a catalytic active centre can serve the surface defects. Oxidation of organic compounds using oxidic catalysts can proceed with alternate reduction and oxidation of catalyst surface. Oxygen from surface layer reacts with organic molecule submitting to oxidation and release as a part of organic molecule. Surface ions of metal are uncovered and can be coordination saturated with oxygen from ambient atmosphere (in case of friction process or thermogravimetry), or with oxygen penetrating to the polymer structure, as can be supposed during crosslinking process.

The key role in the phenol–formaldehyde resin degradation process can be attributed to the elimination of formaldehyde caused by metal as well as metal oxide catalysis.

Brass (CuZn) does not influence the degradation regardless of concentration but the wear rates of brass containing samples were extremely high if compared to copper and iron containing samples. It can be considered that brass influence is rather physical owing to formation of ZnO and consequent weakening of fiber/resin interface. The catalytic inactivity of brass can be attributed to the presence of zinc in copper lattice. With addition of zinc in copper lattice, the concentration of electrons in primary alloy increases. Consequently, the copper ions Cu^{2+} in surface layers are reduced to catalytically inactive copper form Cu^{+} and Cu^{0}.

Acknowledgements

This research was supported by the NSF grant No. EEC9523372 and the Ministry of Education of Czech Republic grants No. CEZ 279000017 and ME 343.

References

[1] Saunders KJ. Organic polymer chemistry. London: Chapman and Hall; 1973.
[2] Conley RT, Guadiana RA. Thermal stability of polymers, Vol. 1, New York: Marcel Dekker Inc.; 1970.
[3] Costa L, Rossi di Montelera L, Camino G, Weill ED, Pearle EM. Structure–charring relationship in phenol–formaldehyde type resins. Polymer Degradation and Stability 1997;56:23–35.
[4] Yamashita Y, Ouchi K. A study on carbonization of phenol – formaldehyde resin labelled with deuterium and ^{13}C. Carbon 1981;19:89–94.
[5] Trick KA, Saliba TE. Mechanisms of the pyrolysis of phenolic resin in a carbon/phenolic composite. Carbon 1995;33(11):1509–15.
[6] Hetper J, Sobera M. Thermal degradation of novolac resins by pyrolysis-gas chromatigraphy with a movable reaction zone. Journal of Chromatography A 1999;833:277–81.
[7] Roman-Martinez MC, Cazorla-Amoros D, Linares-Solano A, Salinas-Martinez de Lecea C, Atamy F. Structural study of phenolformaldehyde char. Carbon 1996;34(6):719–27.
[8] Ouchi K, Honda H. Pyrolysis of coal I—Thermal cracking of phenolformaldehyde resins taken as a coal models. Fuel 1959;38:429–43.
[9] Heron GF. High temperature resistance and thermal degradation

of polymers. New York: Society of Chemical Industry, GORDON and BREACH Sci publishers; 1961.
[10] Manfredi LB, Osa O, Fernandez NG, Vazquez A. Structural – properties relationship for resols with different formaldehyde/phenol molar ratio. Polymer 1999;40:3867–75.
[11] Morterra C, Low MJD. IR studies of carbons - VII. The pyrolysis of a phenol–formaldehyde resin. Carbon 1985;23(5):525–30.
[12] Knopp A, Pilato LA. Phenolic resin, chemistry, applications and performance. Berlin: Springer-Verlag; 1985.
[13] Rao MR, Alwan S, Scariah KJ, Sastri KS. Thermochemical characterization of phenolic resins. Journal of Thermal Analysis 1997;49:261–8.
[14] Smrčok L, Weiss Z. J Appl Cryst 1993;26:140–1.
[15] Weiss Z, Krajíček J, Smrčok L, Fiala J. J Appl Cryst 1983;16:493–7.
[16] Hair JF. Multivariate data analysis. Upper Saddle River: Prentice Hall; 1998.
[17] Morrison RT, Boyd RN. Organic chemistry, Fourth edition, Allyn and Bacon, 1983.
[18] Holopainen T, Alvila L, Rainio J, Pakkanen TT. IR spectroscopy as a quantitative and predictive analysis method of phenol – formaldehyde resol resin. Journal of Applied Polymer Science 1998;69:2175–85.
[19] Kuthan J. Organic chemistry II. Prague: VŠCHT; 1988 (in Czech).
[20] Koubek J, Kraus M, Schneider P. Technical catalysis I. Prague: VŠCHT; 1990 (in Czech).
[21] Shinohara Y, Satozono H, Nakajima T, Suzuki S, Mishima S. Study of the interaction of ethanol with the Broensted and Lewis acid sites on metal oxide surfaces using the DV—Xα method. Journal of chemical software 1997;4(2):41–9.
[22] Greenwood NN, Earnshaw A. Chemistry of elements II. Oxford: Pergamon Press Plc; 1993.